The Scattering of Protons by Protons near 30 Mev, Photographic Method*

WOLFGANG K. H. PANOFSKY AND FRANKLIN L. FILLMORE
Radiation Laboratory, Department of Physics, University of California, Berkeley, California
(Received February 20, 1950)

The scattering of 29.4-Mev protons by hydrogen gas at one atmosphere pressure has been studied with the beam of the Berkeley linear accelerator. The beam, collimated to a diameter of $\frac{1}{16}$ in., passes through the gas and constitutes a line source of scattered protons. The scattering angle of the scattered protons is measured directly in the emulsion of 50μ Ilford C-2 emulsions. Measurements of the range of the scattered protons was made on a fraction of the tracks. From range-energy relations established in the magnetic field of the 184-in. cyclotron for the emulsions used, the primary energy of the protons before scattering was found to be 29.4 $\pm$0.1 Mev. Protons were observed in the angular range $10° \leqslant \theta_{lab} \leqslant 80°$; two independent sets of scattering data in the angular region greater or less than 45° are thus obtained; a valuable internal check on observational errors or background or impurity effects is thus possible. No statistically significant difference in the two regions was observed. 10,934 tracks have been tabulated; this results in the statistical error approximately matching systematic errors such as those due to tolerance of plate geometry, observational error, etc. Cross sections obtained are absolute; the beam is measured by absorption in a Faraday cup and charge integration on a low leakage condenser. The most significant result of these experiments is the apparent absence of expected repulsive P wave and of D wave effects.

I. INTRODUCTION

THE scattering of protons by protons has been studied by many observers[1–15] covering an energy range up to 14.5 Mev,[9] and recently at 240 Mev[14] and 340 Mev.[15] Unfortunately, the accuracy of the experiments in the region above 7 Mev and below this work has not been sufficient to permit significantly different conclusions to be drawn as compared to the conclusions obtained from the more precise low energy experiments. With possible small deviations all low energy experiments can be interpreted[16] in terms of scattering in the lowest state of angular momentum only. As has been shown by Schwinger,[17] Blatt,[18] and others[19] this permits the determination of only two parameters of an assumed potential of interaction between the particles. The essential conclusion drawn from these experiments is the fact that these parameters calculated from the $p-p$ S wave interaction are essentially the same as the parameters calculated for the $n-p$ S wave interaction in the singlet state.

This investigation was undertaken in order to extend $p-p$ scattering data into the region where the contribution from scattering in higher states of angular momentum should certainly become significant. The protons used in this experiment were produced by the Berkeley linear accelerator. This accelerator provides a beam up to an energy of 32 Mev, the beam being of small diameter and small angular divergence and thus

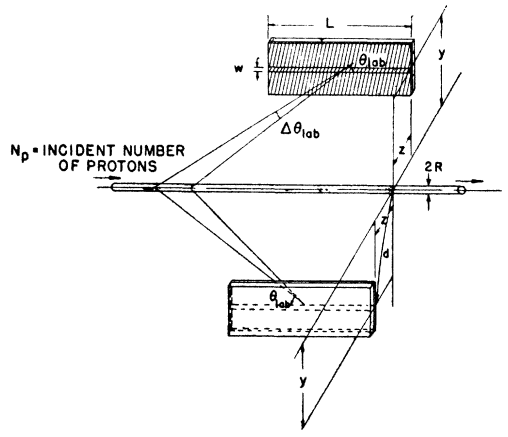

FIG. 1. Relative geometry of a photographic plate "pair" to the beam. Geometrical parameters shown are: L=length of swath scanned; W=swath width; Z=off-set of emulsion surface from beam center line; y=distance of swath from plane through beam normal to emulsion surface; $d=(Z^2+y^2)^{\frac{1}{2}}$=distance of beam center line to swath; R=beam radius; θ_{lab}=laboratory scattering angle.

* This work was done under the auspices of the AEC.
[1] W. H. Wells, Phys. Rev. **47**, 591 (1935).
[2] M. G. White, Phys. Rev. **49**, 309 (1936).
[3] Tube, Heydenburg, and Hafstad, Phys. Rev. **50**, 806 (1936); 600–900 kev.
[4] Hafstad, Heydenburg, and Tuve, Phys. Rev. **53**, 239 (1938).
[5] Heydenburg, Hafstad, and Tuve, Phys. Rev. **56**, 1078 (1939); 867, 680, 776 kev.
[6] Herb, Kerst, Parkinson, and Plain, Phys. Rev. **55**, 998 (1939); 860, 1200, 1390, 2105, 2392 kev.
[7] R. R. Wilson, Phys. Rev. **71**, 384 (1947); 10 Mev.
[8] R. R. Wilson and E. C. Creutz, Phys. Rev. **71**, 339 (1947); 10 Mev.
[9] Wilson, Lofgren, Richardson, Wright, and Shankland, Phys. Rev. **71**, 560 (1947); 14.5 Mev.
[10] Dearnley, Oxley, and Perry, Phys. Rev. **73**, 1290 (1948); 7 Mev. J. Rouvina (private communication).
[11] Blair, Freier, Lampi, Sleator, and Williams, Phys. Rev. **74**, 553 (1948); 2.42, 3.04, 3.27, 3.53 Mev.
[12] Ragan, Kanne, and Taschek, Phys. Rev. **60**, 628 (1941); 176 and 200 kev.
[13] Bondelid, Bohlman, and Mather, Phys. Rev. **76**, 865 (1949); 5.11 Mev.
[14] C. L. Oxley, Phys. Rev. **76**, 461 (1949), 240 Mev.
[15] O. Chamberlain and C. Wiegand, Phys. Rev. **79**, 81 (1950).
[16] For a review of the present state of the interpretation of $p-p$ scattering experiments see: H. A. Bethe, Phys. Rev. **76**, 38 (1949); also J. D. Jackson, M.I.T. Tech. Report No. 29 (July 15, 1949); also Jackson and Blatt, Rev. Mod. Phys. **22**, 77 (1950).
[17] J. Schwinger, Phys. Rev. **72**, 742(A) (1947); lecture notes on nuclear physics, Harvard (1947). (As quoted by Blatt and Jackson, reference 18.)
[18] J. M. Blatt, Phys. Rev. **74**, 92 (1948) and J. M. Blatt and J. D. Jackson, Phys. Rev. **76**, 18 (1949).
[19] J. Smorodinski, J. Phys. U.S.S.R. **8**, 219 (1944); **11**, 195 (1947).

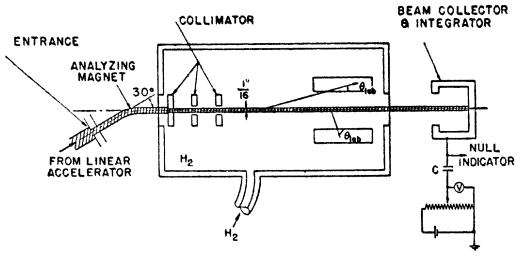

FIG. 2. Schematic layout of collimating system, scattering chamber, and integrator.

well suited to scattering experiments. The authors are greatly indebted to the members of the linear accelerator crew for their efficient operation of the machine during the bombardments.

It was felt that the importance of the problem of $p-p$ scattering in the 30-Mev range justified that the experiments be performed by two entirely independent methods. Cork, Johnston, and Richman[20] have undertaken the study by means of a proportional counter method; their methods and results are given in an adjoining paper. This paper describes the results obtained by means of an apparatus using photographic plates as detectors. The results reported here are not final; it was felt, however, since most of the theoretical implication of this work does not rest on the features requiring the highest attainable accuracy, that publication at this stage of the work was advisable.

II. DESCRIPTION OF APPARATUS

A. Ideal Geometry

The first use of photographic plate techniques in the study of $p-p$ scattering was made at the University of Rochester[10] at 7 Mev. In the Rochester experiment an annular exit slit was employed which resulted in a one to one correspondence between track position and scattering angle. This reduced analysis of the plates to a simple counting operation. The problems associated with slit scattering and penetration to be expected at 30 Mev led us to adopt the more laborious method, namely of actually measuring the scattering angle of all tracks directly in the emulsion. The method is made practical in this energy region by the small multiple Coulomb scattering in the emulsion. Range measurements were also made whenever the track length permitted us to do so. This permitted an internal check as to the primary energy.

The proton beam from the linear accelerator is first monochromatized and collimated to $\frac{1}{16}$ in. diameter by means of equipment described below. The beam then passes into the scattering chamber in which plates are disposed symmetrically about the beam in the manner shown in Figs. 1 and 2. The solid angle subtended by a swath of width W and length L parallel to the beam is then directly defined by the distance d from the swath to the centerline of the beam and the offset Z of the plane of the emulsion and the beam. It is easily shown by elementary calculation that, if the finite beam size is ignored, the number of tracks N_t for a given number of incident protons N_p is given by

$$\frac{N_t}{N_p}=N_v\left(\frac{d\sigma}{d\omega}\right)_{cm}\frac{WLZ}{d^2}\frac{\Delta\omega_{cm}}{2\pi}, \tag{1}$$

where N_v is the number of scattering centers per unit volume and $(d\sigma/d\omega)_{cm}$ is the differential cross section in the center-of-mass coordinates. $\Delta\omega_{cm}$ represents the increment of solid angle in the center-of-mass frame corresponding to the range $\Delta\theta_{\rm lab}$ in the laboratory angle $\theta_{\rm lab}$ within which the N_t tracks have been recorded. This equation can be written in the equivalent form

$$\frac{N_t}{N_p}=N_v\left(\frac{d\sigma}{d\omega}\right)_{cm}\frac{WLZ}{d^2}\Delta\,(\cos 2\theta_{\rm lab}), \tag{2}$$

which forms the basis for all cross-section computations. It is to be noted that in this simple geometry the number of tracks corresponding to a given interval in solid angle is simply proportional to the differential cross section without any further angular dependence.

B. Non-Ideal Geometry—Design of Plate Holder

The scattering geometry depends linearly on the offset Z of the emulsion face toward the beam center. In the apparatus as described here $Z\cong 0.070$ in. and therefore if data were based on the tracks as measured in a single plate, an excessive dependence of the calculated absolute cross section on beam position would result. To obviate this difficulty the plates were arranged in a symmetrical array about the beam center. Figure 1 shows one pair of plates only. It is easy to show that if the measurement of cross section is based on the *sum* of the tracks measured in paired plates (see Fig. 1),

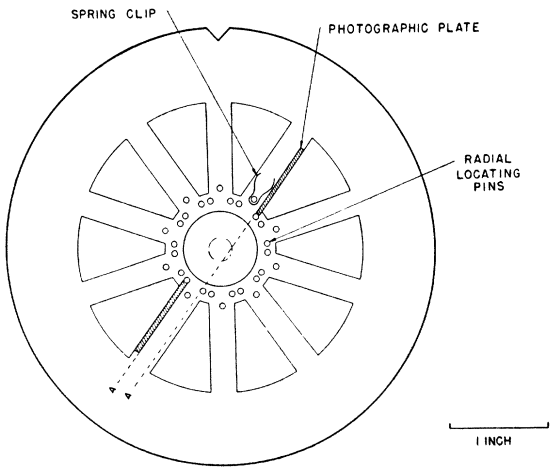

FIG. 3. Diagram of base plate of cartridge showing the means of radial and azimuthal localization of the plates. The distance $A-A$ corresponds to the interface distance D of Eq. (4).

[20] Cork, Johnston, and Richman, Phys. Rev. **79**, 71 (1950).

then the fractional error ϵ_Z due to an error δ_Z in beam centering parallel to Z is given by

$$\epsilon_Z = 3(\delta_Z)^2/(y^2+Z^2), \tag{3}$$

while the fractional error ϵ_D due to an error δ_D in the face to face distance D between the emulsion faces is given by

$$\epsilon_D = \delta_D/D \tag{4}$$

and the error ϵ_y due to an error δ_y in y, where $2y$ is the edge-to-edge distance between paired plates, is given by

$$\epsilon_y = 2\delta_y/y. \tag{5}$$

The ratio between the number of tracks recorded in the two members of a pair of plates depends linearly on the off-center displacement of the beam. If N_1 and N_2 are the tracks recorded in the two members of a pair, it is easy to show that

$$(N_1-N_2)/(N_1+N_2) = \delta_Z/Z \tag{6}$$

and hence

$$\epsilon_Z = [(N_1-N_2)/(N_1+N_2)]^2 \cdot [3Z^2/(y^2+Z^2)]. \tag{7}$$

The error in absolute cross section due to lack of beam centering can thus be evaluated directly by an internal check on the symmetry of the track counts. Experimentally it has been possible to keep the error ϵ_Z well below 0.1 percent corresponding to a centering error δ_Z of less than 0.01 in. A similar calculation can be made on the effect of beam centering in the y direction. It is to be noted that this, and other possible geometrical errors, have no bearing upon the relative cross section but only on the absolute measurements.

The errors ϵ_D and ϵ_y are independent of beam position and are only dependent on the accurate *relative* location of the plates. To achieve this required accuracy, a precision plate holder-cartridge was machined out of Lucite and Duraluminum. Figure 3 shows the base diagram of the cartridge end plates. The faces $A-A$ are held to a tolerance of ± 0.0005 in. by means of go/no-go gauges which were applied before and after every run. The cartridge was designed to hold up to 20 plates for simultaneous exposure. This design was adopted during the initial stages of testing of the Berkeley linear accelerator when it appeared that the proton beam current might be very small. Since the current is now more than adequate for this experiment only six of the plate positions are occupied. It also seemed inadvisable to place plates with their emulsions facing one another, since calculation shows that the probability of a proton scattering out of one emulsion face and entering the opposite emulsion cannot be considered negligible.

In addition to the precision gauging of the distance $A-A$ (Fig. 3), precise determination of the face to face distance requires also knowledge of the photographic plate glass thickness and flatness and also knowledge of the emulsion thickness. The plates were measured after processing to ± 0.0004 in. using surface plate and dial gauge equipment. A correction was applied for emulsion shrinkage using a shrinkage factor of 2.0. Since the emulsion thickness used is only $50\mu = 0.002$ in., the uncertainty in shrinkage factor produces negligible error.

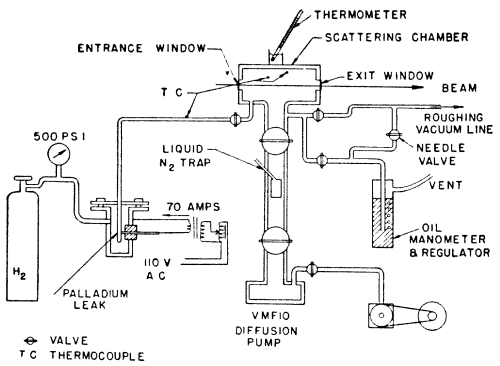

FIG. 4. Schematic diagram of gas handling system. Oil manometer and regulator regulates H_2 pressure and meters it against atmospheric pressure.

The plates are held onto the cartridge precision faces by means of light springs which assure positive contact with the surfaces $A-A$. The cartridge is always kept either in vacuum or in a desiccator to avoid possible warping due to moisture absorption.

The cartridge is centered in the barrel of the gas handling system by means of six steel balls, two of which are spring-loaded, thus providing a correct kinematic support. The collimator (see Fig. 2) is aligned with the barrel to within ± 0.004 in. As a result of this, it is assumed that if the beam is centered at one point of the scattering volume, it is centered at all points. The final centering of the beam is made by adjusting the analyzing magnet current and checking with a fluorescent screen. The final criterion as to centering does of course rest on the actual track count as outlined above.

Equation (2), on which the cross-section calculations are based, is strictly true only if the incoming beam constitutes an ideal line source. Errors caused by the finite diameter of the beam have been investigated in detail. The result is as follows. If the radius of the beam is R, then the ideal formula Eq. (2) is multiplied by a correction factor of

$$1+\tfrac{1}{4}(R/d)^2[\cos\theta_{cm}(\cos\theta_{cm}-1)-\tfrac{1}{2}] \tag{8}$$

where the integration over the beam has been carried out under the assumption that the differential cross section is constant over the range of integration. Since R is of the order of $\frac{1}{32}$ in. and $d>0.500$ in. this correction never exceeds 0.15 percent for all angles and is therefore negligible.

The finiteness of the scattering length of the beam does not introduce a correction but simply introduces limits on the range of angles which can be considered as originating in the gas. This restricts the smallest

angle which can be read unambiguously to 3° on the inner edge of the plate and to 8° on the outer edge. In practice angles were read in the interval:

$$10° \leq \theta_{lab} \leq 80°. \quad (9)$$

A further small geometrical error worth considering is the obliquity of incidence of the protons on the photographic emulsion. An elementary calculation, which also takes into account the finite width of the beam, shows that this error cannot exceed 0.1° and is usually much less. This source of error has thus been neglected.

A further deviation from "ideal" geometry which has been considered is the probability that a proton will enter the emulsion, then scatter back out again and re-enter the emulsion at a "hill" in the emulsion. This effect can be estimated with knowledge of the waviness of the emulsion. A microscopic measurement was made of the flatness of unprocessed emulsion surfaces and it was found that the "waviness" amounts to less than 1μ in height per 150,000 sq. μ of emulsion surface. By combining this information with calculation of the emulsion scattering, this effect appears negligible.

C. Vacuum and Gas Handling System

The hydrogen scattering chamber is separated from the linear accelerator vacuum by means of an entrance window, $\frac{1}{4}$-in. diameter, made of 0.001-in. aluminum.

The chosen operating pressure of H_2 was one atmosphere; for 30-Mev protons the broadening of the beam due to multiple scattering in the chamber is only 0.011 in. Multiple Coulomb scattering of sufficient magnitude to enter the plates is thus excluded. The nuclear cross sections are sufficiently small such that plural nuclear events are excluded also.

Figure 4 shows a schematic diagram of the gas system. In a $p-p$ scattering experiment with a gas target one of the main problems is that of gas purity; at this energy however, this problem is of course less significant than at lower energy since the Coulomb cross section falls off faster with energy than the nuclear scattering yields. The principal source of impurities proved to be water vapor or other contaminants evolved from the photographic plates themselves. Since the scattering angles cover the range of $10° \leq \theta_{lab} \leq 80°$ it was possible to check the presence of impurities by an asymmetry of tracks about a laboratory angle of 45°. These tests indicate that it was necessary to dehydrate the plates for at least four hours in high vacuum before data could be taken. Figure 5 shows a typical dehydration curve of the plates, showing that after a pump-out time of four hours the partial pressure of impurities would not rise to more than 0.05 percent of the total pressure in a 30-min. bombardment.

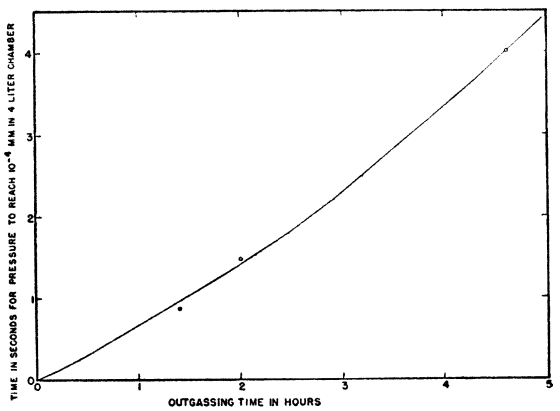

FIG. 5. Outgassing curve of 50μ Ilford C-2 plates during typical run. The accumulated impurity contribution during a run is estimated from this type of data.

Considerable trouble was encountered from peeling of the emulsion from the glass surface when this outgassing procedure was used. After many unsuccessful experiments to reduce peeling by taping the emulsion edges, covering the plates with collodium, etc., an emulsion (Ilford C-2; 50μ thickness, Emulsion No. Z2199) was found which withstood the outgassing treatment without peeling difficulties. All attempts to use Eastman-Kodak NTB emulsions proved unsuccessful.

After pump-out the scattering chamber was isolated from the pump and liquid nitrogen trap (to preserve thermal equilibrium) and hydrogen was admitted through a palladium leak. This leak (Fig. 6), designed by Mr. L. Johnston and Mr. E. A. Day, consists of a palladium tube of $\frac{1}{4}$-in. diameter and 0.006-in. wall thickness, internally supported by ceramic rings. It was heated to a temperature slightly below red heat by passing a current of approximately 70 amp. directly through the tube, corresponding to a dissipation of approximately 250 watts. The external pressure was maintained at a pressure of 500 p.s.i. of H_2. At this pressure differential the chamber (volume $\sim$4 liters) could be filled in 20 min. to a pressure of one atmosphere. The leak was outgassed by heating in vacuum before every run and tested for imperviousness to gases other than hydrogen by an external helium atmosphere.

The pressure was maintained at a constant pressure differential against atmospheric pressure by means of an oil-filled manometer which simultaneously served as a pressure regulator. During the run the palladium leak was operated continuously thus changing the H_2 gas once every 20 min. Most of the gas was removed by a vacuum pump throttled by a needle valve; a slight excess bubbled out through a manometer-regulator. The density of the oil in the manometer ("Litton" diffusion pump oil) was determined by weighing. The pressure excess used was of the order of 10 in. of oil, i.e., only two percent of the total pressure. The atmospheric pressure was read to 0.1 mm on a precision mercurial barometer. Difference in altitude between locations of the barometer and scattering chamber introduced a correction of 0.6 mm of Hg.

The gas temperature was read by means of an accurate thermometer in contact (maintained by a water cup) with the heavy brass barrel containing the gas and plate cartridge. The only question then is whether the beam barrel is in temperature equilibrium with the gas. This point was investigated by introducing thermocouples into the hydrogen gas and onto other points. Couples were located: (1) near the center of the vessel in the scattering region; (2) at the outer edge of the hydrogen volume; (3) along the copper tubing leading hydrogen into the chamber. The three couples showed differentials corresponding to less than 1°C. One of the couples was surrounded by a radiation shield consisting of a polished aluminum cylinder; presence or absence of this shield did not affect the temperature readings. Problems regarding temperature equilibrium appear to be insignificant here, as contrasted to earlier work on this subject; the reason is presumably the high pressure of hydrogen used.

D. Beam Collimation

In any high energy experiment of this kind the principal concern is the reduction of background. "Background" tracks observed were principally attributed to the following causes: (1) slit scattering on collimator apertures; (2) particles starting from chamber walls and from plate holders; (3) protons generated by $n-p$ collisions in the chamber gas; and (4) neutron knock-ons and neutron-induced nuclear processes in the emulsion. Let us now discuss the various measures taken to reduce the sources of background.

Figure 7 shows the relative disposition of collimator and the photographic plates. Two considerations affect the choice of collimator material: one is the neutron production in the collimator parts, and the other is the fraction of incident protons which will scatter out of the slit after having penetrated the material. The first point makes carbon a logical choice: the total yield for neutron production in carbon is only approximately 10^{-3} at 30 Mev and the energetic upper limit on the possible neutron energy is 10 Mev. This means that a

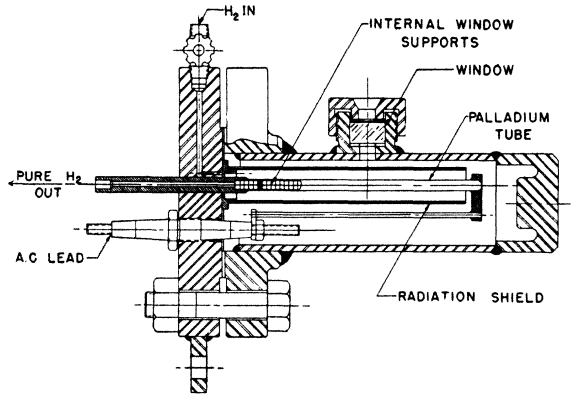

FIG. 6. Diagram of 500 p.s.i. external pressure palladium leak. Note that the palladium tube is directly heated.

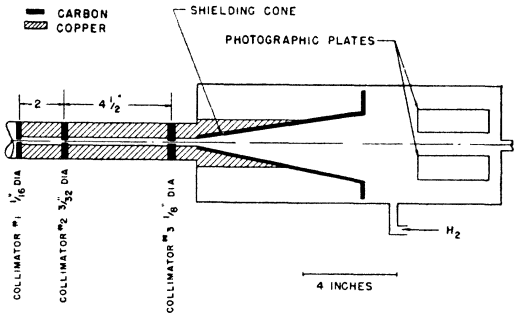

FIG. 7. Diagram of collimating system.

neutron formed on carbon does not have sufficient energy to produce a nuclear reaction when impinging on graphite. Accordingly, the collimating disks were made of graphite and in addition the faces of the plate holder which could "see" the photographic plates were lined with graphite. As to the second point, namely the problem of the proton scattering out of the slit after initial penetration, calculations† show that if the edges of a carbon slit of full range thickness is hit by a beam of 30-Mev protons, an amount will scatter out of the slit corresponding to the number of protons incident over a strip of width 0.001 in. For lead the corresponding number is 0.007 in. A low atomic number collimating disk is thus of advantage here. From this point of view either Be or C are favored; however, the small neutron binding energy in Be makes the choice of carbon the most reasonable. It is essentially impossible to design a collimator such that no secondary protons can reach the photographic plates; the present design (Fig. 7) simply minimizes the slit scattered protons, consistent with a given length of collimator. The number of slit-scattered protons can of course be further reduced by lengthening of the collimator, however at the expense of decreased mechanical tolerances. There are still a large number of slit scattered tracks on the plates (for statistics see Section III-B) but these cannot fall on the plates at an angle exceeding 8° and are therefore not included in the tabulation range.

In order to attenuate the neutron flux through the scattering regions and the region of the plates, the collimating disks were surrounded by copper pieces. Copper has a mean free path of approximately 4 in. for inelastic events for fast neutrons and hence appreciable flux reduction is possible. Also an additional 2-mm aperture was introduced ahead of the analyzing magnet (see Fig. 2) which reduced the number of protons incident on the collimator and hence reduced the neutron flux.

One of the effects of neutrons in the hydrogen chamber is to produce $n-p$ collisions resulting in erroneous proton tracks. In order to reduce the hydrogen volume "seen" by the plates a cone turned of graphite was intro-

† This calculation was made by E. A. Martinelli, to whom the authors are indebted.

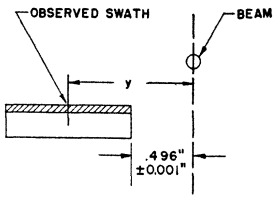

FIG. 8. Measurement of y.

duced to cut off the hydrogen region not traversed by hydrogen scattered protons (see Fig. 7).

It should be pointed out that the efficacy of the background reduction measures does not have to be evaluated by calculation but is experimentally determined both by background runs and by the symmetry of tabulated tracks about a laboratory angle of 45°. (See Sections III and V.)

E. Integrator

The beam, after passage through the scattering chamber is integrated by collection in a Faraday cup. The integrator was constructed by Mr. Lee Aamodt. The charge is collected on a low leakage condenser. Details of construction of the instrument, the method of calibration and the test for secondary emission are described in the adjoining report by Cork, Johnston, and Richman.[20]

III. TECHNIQUE OF GATHERING DATA

A. Microscope Technique

The plates are scanned under a high power microscope to count the number of scattered proton tracks. A 97x oil immersion objective is used with 7.5x eyepieces. The data required are the angle θ_{lab} and the distance d of the entering point of the track from the beam center. We recorded θ_{lab} and the coordinates x_0, y_0 of the point where the track enters the emulsion. x_0 was recorded to enable one to relocate individual tracks when checking the counting which another person has done; this will be discussed later. The actual recording is done by photographing the readings of three rotary counters which are connected to the microscope drives by flexible shafts. A Recordak Jr., Model J.C. microfilm recorder‡ was rented for this purpose, and the three counters placed on the stage of the microfilm recorder. One eyepiece has a specially built worm drive attachment so that it can be rotated for measuring the angle of the scattered proton tracks. It has a reticle with a hair line ruled on it for this purpose as well as a scale representing a length of 100μ (actually 102.0 $\pm$0.5μ) so that ranges of tracks can be measured accurately. The other eyepiece has two accurately parallel hair lines which correspond to a separation of 127.0 $\pm$0.5μ. Tracks which enter the emulsion between these lines are counted, so that a swath 127μ wide the length of the plate is read at one setting of the microscope carriage y coordinate.

The plate holder on the microscope carriage was designed and constructed by W. W. Brower to permit very accurate alignment of the plates in the microscope and accurate re-inserting of a plate if it has to be removed from the microscope at any time. Plates were re-inserted accurately in the plate holder to closer than 0.001 in. after a 6-month interval. The plate is clamped securely by a spring which presses it against two indexing ledges, one at each end of the plate, which correspond in position to the indexing surfaces in the scattering chamber plate holder. These indexing ledges were observed to be accurately parallel to the axis of the lead screw on the microscope carriage x coordinate drive to within 1/1000 of a radian. The hair line in the goniometer eyepiece can be set parallel to these indexing ledges to within 3/1000 of a radian. The accuracy of its alignment is checked every few hundred tracks to insure that the mechanism has not slipped. Thus any systematic error in measuring θ_{lab} is less than 0.2°.

The rotary counter which records θ_{lab} can be read to 0.1°. Back-lash in the mechanism is less than 0.3°. The vernier scale on the x and y coordinate lead screws of the microscope carriage are graduated in thousandths of an inch and were checked against a Bausch and Lomb standard showing that they were accurate to closer than one part in a thousand. The separation of inside plate edges of paired plates in the scattering chamber plate holder was measured to be 0.992$\pm$0.002 in. The y distance from the axis of the geometry to the center of a swath is obtained by adding half of 0.992 in. to the distance from the edge of the plate to the center of the swath as read from the y coordinate of the microscope. Thus the distance y to the center of a swath is measured to within about $\pm$0.001 in. (See Fig. 8.)

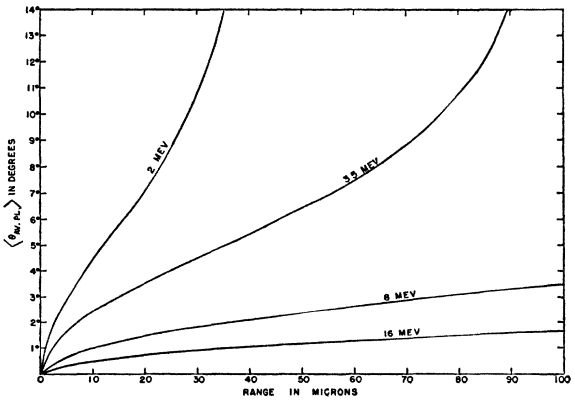

FIG. 9. Plane projected root mean square scattering angle plotted as a function of the distance along a proton track. Various primary energies are shown. This scattering angle is the r.m.s. of the plane projection of the angle of the tangent to the track with the initial direction.

‡ Can be rented from: Recordak Corporation, 561 Clay Street, San Francisco, California·

B. Criteria for Reading Tracks

When one looks at a plate it becomes quite evident that many of the tracks seen are obviously not scattered protons at 30 Mev, but are what we call a non-confusable background. Such tracks are caused by scatterinf from the collimating slits, neutrons producing knock-on protons in the gas and plate holder material, protons scattered backwards from the 1-mil aluminum exit foil, or scattered protons which strike the walls of the chamber and are there scattered through a large angle either elastically or inelastically. The majority of such tracks are non-confusable since they are observed to have quite low energies. This non-confusable background, including slit scattering which enters at $\theta_{\text{lab}}<8°$, is very roughly double in number to the number of good tracks on the plate.

In addition to this obviously non-confusable background, one sees tracks which can easily be mistaken for good scattered proton tracks but which upon more careful consideration can be shown to be spurious. Such tracks are due to the small fraction of the background protons mentioned in the preceeding paragraph which happen to enter the emulsion at an energy very nearly correct for their scattering angle θ. These tracks are about eight percent of the good tracks, and their detection is a matter which requires a fair amount of skill and judgement on the part of the observer. Since it was desired to have several observers counting tracks it was necessary to undertake a training program which would insure that all observers were competant to detect these barely non-confusable tracks and eliminate them. To this end several criteria were established for the judging of each track, and each observer was carefully instructed in their application. Spot checks on the counting of each observer have been made and an estimate of the reliability will be given later. In order to establish the basis for the criteria and also to consider the angular accuracies of this method it is first necessary

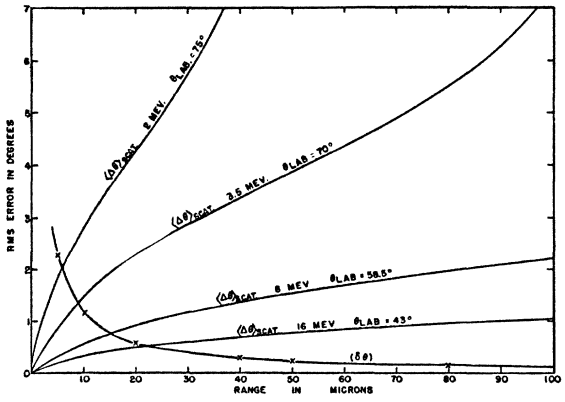

FIG. 10. Root-mean-square error $\langle\Delta\theta\rangle_{\text{scat}}$ in measuring θ_{lab} due to scattering, obtained by comparing the direction from the point of entry to a point along the track with the initial direction, plotted as a function of range. Also shown is the error $\langle\delta\theta\rangle$ in measuring θ_{lab} due to finite grain size, plotted as a function of the length of track used in making the measurement.

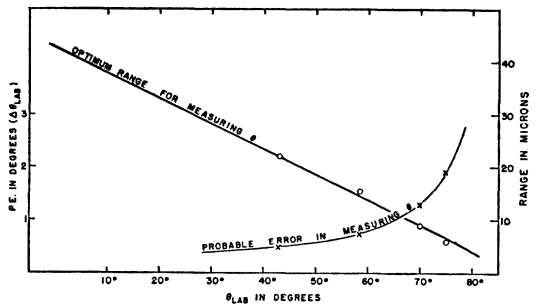

FIG. 11. Plot of optimum range for angle measurement as obtained equalizing scattering and grain size errors. The resulting over-all probable error $\Delta\theta_{\text{lab}}$ is also shown.

to investigate the multiple scattering of protons in the emulsion.

The mean square of the plane projection of the scattering angle of a particle of unit charge, momentum p and mass m, traveling a distance x in an absorber of atomic number Z and numerical density N is[21,22]

$$\langle\theta_{\text{Av.pl.}}\rangle^2=(4\pi e^4Z^2Nx/p^2v^2)\ln(\theta_{\max}/\theta_{\min}) \quad (10)$$

where $\theta_{\min}=mcZ^{\frac{1}{3}}/p181=\lambda Z^{\frac{1}{3}}/137^2r_0$ is given by screening and $\theta_{\max}=\lambda/(0.57r_0Z^{\frac{1}{3}})$ is given by the finite size of the nucleus. Thus Eq. (10) can be written (nonrelativistically)

$$\langle\theta_{\text{Av.pl.}}\rangle^2=[2\pi r_0^2/(E/mc^2)^2]xNZ^2\ln(181Z^{\frac{1}{3}}) \quad (11)$$

where $r_0=2.82\times10^{-13}$ cm, m is the electron mass, and E is the energy and is assumed constant along the path. The composition of the Ilford C-2 emulsions used is given in an article by J. H. Webb.[23] The result of summing Eq. (11) over the components of the emulsion is found to be

$$\langle\theta_{\text{Av.pl.}}\rangle^2=19.7x/E^2 \quad (12)$$

where x is in cm and E is in Mev. The square root of Eq. (12) can be interpreted as the slope of a trajectory after having undergone the r.m.s. scattering. Since E will vary along the path, we must find $\langle\theta_{\text{Av.pl.}}\rangle$ as a function of x by a numerical integration along the path (Fig. 9). We can then find the mean displacement y as a function of x by a numerical integration. The measurement of the scattering angle θ_{lab} is done by measuring the secant over a certain optimum length x of track. The r.m.s. error is this measurement due to scattering will thus be

$$\langle\Delta\theta\rangle_{\text{scat}}=\arctan(y/x). \quad (13)$$

A plot of $\langle\Delta\theta\rangle_{\text{scat}}$ *vs.* x for various energies is shown in Fig. 10.

The determination of the optimum length of track for measuring θ_{lab} will now be discussed. There will be an error in θ_{lab} due to inaccuracy in setting the goniometer eyepiece hair line. This is due to finite width of the

[21] B. Rossi and K. Greisen, Rev. Mod. Phys. **13**, 240 (1941).
[22] H. A. Bethe, Phys. Rev. **70**, 821 (1946).
[23] J. H. Webb, Phys. Rev. **74**, 511 (1948).

TABLE I. Typical data.

Plate	Length scanned	Total tracks	Good tracks	Spurious tracks: Tracks obviously not confusable	Spurious tracks: Grain density wrong	Spurious tracks: Dives too steeply	Spurious tracks: Angle inconsistent with range
P190	0.222 in.	83	35	45	2	1	0
P191	0.355 in.	131	39	90	1	1	0
P192	0.450 in.	149	67	77	1	3	1
P193	0.291 in.	179	35	139	2	3	0
P194	0.292 in.	170	44	121	2	3	0
P195	0.300 in.	132	44	85	0	3	0

hair line and grain diameter. The value we adopt for for this error is

$$\langle\delta\theta\rangle = d/2x \tag{14}$$

where d is the grain diameter which is about 0.3μ according to Webb[23] while we obtained a slightly higher value, namely about 0.46μ, using formulas he gives. We will use the value 0.4μ for d. Values of $\langle\delta\theta\rangle$ are plotted in Fig. 10 along with those of $\langle\Delta\theta\rangle_{\text{scat}}$. In order to minimize the error in angular measurement we must adjust x so as to equalize these two errors. A plot of optimum x *vs.* θ_{lab} is given in Fig. 11. The probable error of the angular measurement $\Delta\theta_{\text{lab}}$ is now given by $0.6745\sqrt{2}$ times the value of $\langle\Delta\theta\rangle_{\text{scat}}$ read at the crossing points on the curves in Fig. 10. A plot of $\Delta\theta_{\text{lab}}$ *vs.* θ_{lab} is shown in Fig. 11. We have neglected scattering in the H_2 after proton scattering but this has a negligible effect on the results. An experimental range-angle plot of 130 tracks to be discussed presently shows good agreement with the above values of $\Delta\theta_{\text{lab}}$.

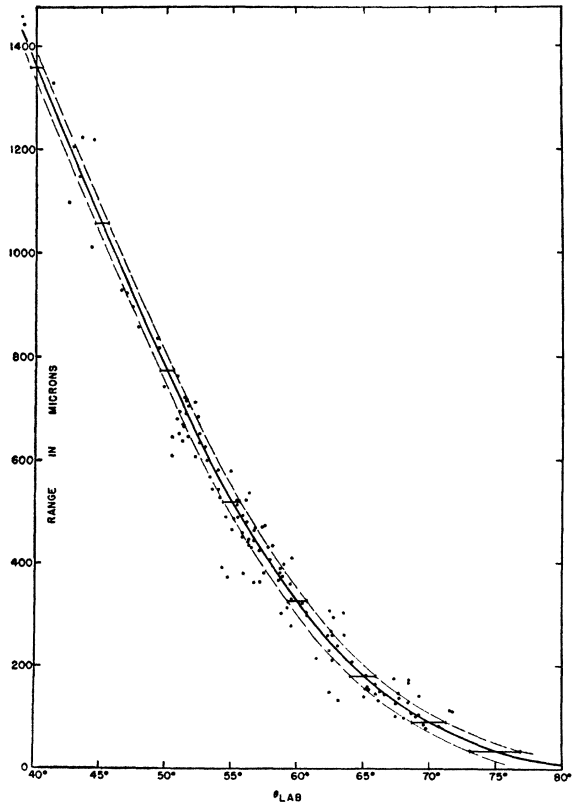

FIG. 12. Plot of the ranges and laboratory scattering angles of 130 protons. The solid line is the best fit for a curve based on a range energy relation of the form $R=\alpha E^{1.72}$ and on the conservation laws. The dashed curves represent the deviation from this curve caused by the probable error in angle measurement as obtained from Fig. 11.

It is evident from Fig. 11 that the probable error in measuring θ_{lab} becomes excessive as θ_{lab} approaches 80°. A more accurate measurement can be made by obtaining θ_{lab} from the experimental range-energy relation of protons in the emulsion used, shown in Fig. 12. The plot contains 130 tracks, and the solid curve represents the best fit based on a range energy relation of the form $R=\alpha E^{1.72}$ which is the range-energy equation given by Bradner *et al.*[24] Since $E\cong E_0\cos^2\theta_{\text{lab}}$, the probable error in θ_{lab} is found to be

$$\Delta\theta_{\text{lab}} = 16.7^\circ\,(\Delta R/R)\cot\theta_{\text{lab}} \tag{15}$$

where ΔR is the probable error in the range measurement. $\Delta R/R$ ranges from about three percent at 65° to about 15 percent at 80°. This gives $\Delta\theta_{\text{lab}}=0.23°$ at 65° and $\Delta\theta_{\text{lab}}=0.44°$ at 80°. While the probable error in angle could be improved by using the range method down to $\theta_{\text{lab}}=60°$ or even lower, the authors decided upon placing the limit at 65° where the error in direct angular measurement is not excessive, because the range measurement is quite time-consuming for the longer tracks.

Since the plates are inclined at a small angle to the beam and the thickness of the emulsion is known, one can calculate the range in which a given proton will dive clear through the emulsion. Let us call this dive distance ξ. The angle β at which a proton enters the emulsion is easily obtained for various θ_{lab} from the geometrical dimensions cited earlier. To β we must add the effect due to scattering in the emulsion, the maximum value for which was taken to be $3\langle\Delta\theta\rangle_{\text{scat}}$. If E is constant along the track, it can be shown that the mean displacement is given by[21,22]

$$\langle y\rangle^2 = \tfrac{1}{3}x^2\langle\theta_{\text{Av.pl.}}\rangle^2, \tag{16}$$

where x is measured along the track, and hence approximately

$$\langle\Delta\theta\rangle_{\text{scat}}\cong[\langle y\rangle^2/x^2]^{\frac{1}{2}}=[\langle\theta_{\text{Av.pl.}}\rangle^2/3]^{\frac{1}{2}}=2.56(x)^{\frac{1}{2}}/E. \tag{17}$$

The unprocessed 50μ emulsion will shrink about 16 percent when dried by evacuation, so we have the following equation to solve for ξ:

$$[\beta+7.68(\xi)^{\frac{1}{2}}/E]\xi=4.2\times10^{-3}\text{ cm}. \tag{18}$$

β was taken at its maximum value over the beam for a given θ_{lab} thus giving the shortest possible ξ. The resulting values of ξ at different positions on the plate are plotted *vs.* θ_{lab} in Fig. 13, which also shows 247 experimental points taken at the center of the plate. On the basis of these points, the minimum value for ξ

[24] Bradner, Smith, Barkas, and Bishop, Phys. Rev. **77**, 462 (1950).

was lowered 15 percent from the theoretical curve and this was used as a criterion in determining which tracks were good. It is thus presumed that if a track dives through the emulsion too steeply it did not come directly from the beam and thus is spurious.

We may now summarize our criteria for determining good tracks. (1) Each track must have $\theta_{lab} \geq 10°$ and $\theta_{lab} \leq 80°$ as determined by a range of 8μ. ($R \geq 8\mu$.) (2) The energy of the track as estimated by its grain density must not be inconsistent with its angle. This is done by visually comparing the grain density of the track in question to the grain density of good tracks at close to the same θ_{lab}. This requires careful judgement on the part of the observer, but since only about three percent of the tracks counted were at all questionable from this point of view the probable error of the results will not be greatly affected by this. (3) For θ_{lab} between 65° and 80° where the grain density criterion is difficult to apply, a better criterion is available; namely, a comparison of range *vs.* angle. If the angle of a track as measured with the goniometer eyepiece disagreed with the angle as determined by the range measurement by more than four times the probable error as computed by the scattering formula above, the track was discarded. (4) Each track had to satisfy the dive distance criterion as discussed in the previous paragraph.

Table I gives a typical sample of the total number of tracks scanned, the number of those accepted as good and the number rejected with the reason for rejection.

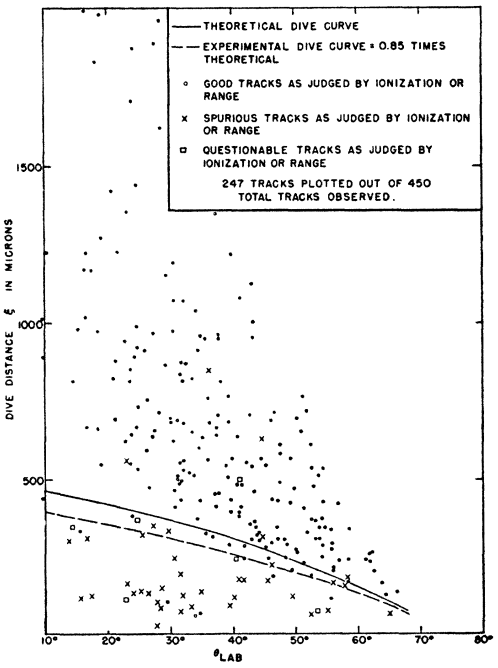

FIG. 13. The range ξ of 247 tracks before "diving" through the emulsion, plotted as a function of laboratory scattering angle. The solid line is the theoretical "limit" of dive distance based on a scattering of three times standard deviation. The dashed line is the experimental "limit curve" used as a criterion for accepting tracks.

It might be remarked here that although this procedure appears to be a somewhat elaborate analysis of the plates, it simply uses fully the information contained in nuclear tracks; namely, track position, ionization, and direction. The rejection of tracks entering at an incorrect angle is equally justifiable as is the selection of a particle trajectory by two counters in coincidence.

C. Background Runs

Since the elimination of all "confusable" background tracks is not possible it is necessary to make some measurements to see how much background is present. The causes of background have already been discussed so we will only describe here the methods of measuring background. Two types of background runs have been made; one, wherein the chamber is kept evacuated during the run, while in the other hydrogen was admitted as in the scattering runs but a graphite tube $\frac{3}{4}$ in. in diameter was inserted axially in the scattering chamber so as to surround the beam and thus prevent scattered protons from reaching the plates. All other geometrical factors were the same as in the scattering runs. These background runs were made immediately after the scattering runs.

Comparison of the counting of tracks on the background runs with that for the scattering runs showed that the high vacuum runs gave about 0.7 percent confusable tracks and the run with the graphite tube gave about 2.1 percent confusable tracks. No angular dependence was observed in the vacuum run. The back-

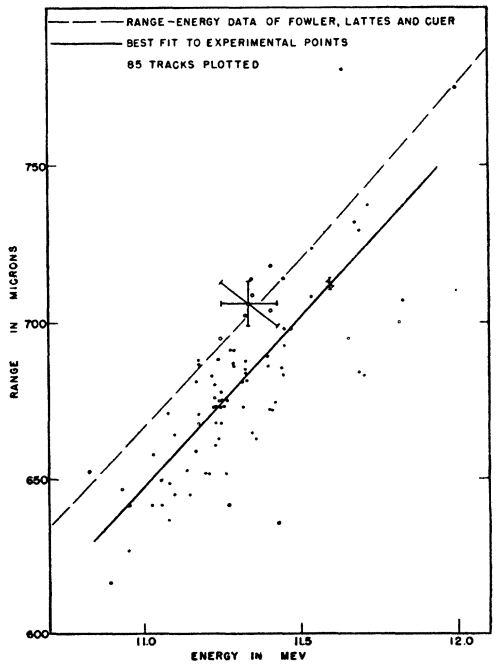

FIG. 14. Ranges and energies of 85 tracks exposed to protons in the 184-in. cyclotron. Emulsions used were the same and received the same treatment as in the $p-p$ scattering runs. Solid line is best fit; dashed line is from the data of Fowler, Lattes, and Cüer.

TABLE II. Run 37.

Original observer	No. of tracks counted	No. of tracks re-counted by F.L.F.	No. of tracks missed	No. of tracks incorrectly counted	No. of tracks which could not be relocated	No. of tracks recorded twice	Net correction per observer (percent)
S.G.A.	894	200	3	4	1	1	+1.5
F.L.F.	5320	610	7	6	1	3	+0.8
W.K.H.P.	1736	253	14	4	3	1	−2.4

ground in the graphite tube run was concentrated toward scattering angle $\theta_{\text{lab}}>50°$. It is believed that the background is due to inelastic events in the carbon and does not represent an applicable correction. The vacuum background has been applied as a correction to the absolute cross section.

IV. PRIMARY ENERGY

The primary energy can be obtained by comparing the measured range of the scattered protons as a function of angle in the emulsion with the experimentally known range-energy relation. In the work of Bradner *et al.*[24] it was found that the relativistically extrapolated range-energy relation given by Fowler, Lattes, and Cüer[25] was essentially correct, but that small variations occur when one compares different emulsion batches. They also found a small effect caused by varying the amount of dehydration of the emulsion just prior to exposure. Because of these variations, the accuracy claimed for the range-energy relation $E=0.251\ R^{0.581}$ given by Bradner *et al.*[24] was ±2 percent. In order to cut down on the error in the energy measurement, the authors have calibrated the emulsion used in this experiment at an energy near that at which comparison with the energy of the scattered protons is to be made. The method used is the same as that described by Bradner *et al.* Plates were exposed in the 184-in. cyclotron after being pumped in the high vacuum of the cyclotron for 6 hr. so that the plates were thoroughly dehydrated just as they were in the scattering runs. The range and energy was measured for 85 tracks and the resulting points plotted on a range-energy diagram, shown in Fig. 14. The data of Fowler *et al.*[25] are shown by the dotted line while the solid line representing the best empirical fit to the experimental points gives ranges which are 2.5 percent below the ranges given by Fowler *et al.*[25]

The probable error in the energy measurement of the proton by radius and field measurements in the cyclotron is found to average 0.8 percent while that of the range measurement is one percent plus 0.95 percent for straggling or a total of 1.4 percent per point. These errors, assumed to be random normal errors, are then combined in the usual manner to give the probable error of the experimental curve, which is thus found to be 0.17 percent. This error is a spread normal to the curves of Fig. 14 and corresponds to 0.24 percent in range.

The experimental range-energy plot for hydrogen scattered protons in this experiment is shown in Fig. 12, where the solid line is the best fit of the form $E=0.251\ R^{0.581}$ (determined empirically by counting the number of points lying above and below the curve), and the dashed curves represent the theoretical probable error $\Delta\theta_{\text{lab}}$ calculated earlier. By counting the number of tracks in the four sections of the graph, we conclude that the theoretical values for $\Delta\theta_{\text{lab}}$ are sufficiently accurate for our needs. The observed range for $\theta_{\text{lab}}=45°$ is 1058μ. When the 2.5 percent experimental correction obtained above is applied to the Fowler *et al.*[25] range-energy data, this corresponds to an energy of 14.59 Mev at the plates. The energy lost in the hydrogen after scattering at 45° is 24 kev, so the energy after scattering at 45° is 14.61 Mev. The relativistically correct formula for the kinetic energy of a scattered proton whose primary energy is E_0 in the lab system is given by

$$E=\frac{E_0\cos^2\theta_{\text{lab}}}{1+(E_0/2Mc^2)\sin^2\theta_{\text{lab}}}. \tag{19}$$

This gives the energy before scattering to be 29.4 Mev.

The probable error of the observed range is seen from Fig. 12 to be $\pm5.4\mu$ or 0.51 percent which when combined with the probable error of the range energy relation gives a total probable error of 0.56 percent for the range; using the exponent in the Bradner *et al.*, range-energy relation this corresponds to a probable error in the primary energy of 0.33 percent or ±0.1 Mev. Note that this represents the probable error of defining the central value of the energy and not necessarily the energy spread. By analysis of the geometry of the analyzing magnet it can be shown that the beam is monochromatic to ±0.18 Mev.

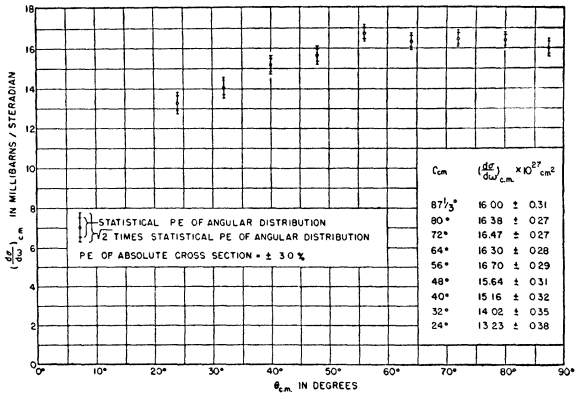

FIG. 15. Observed differential cross section (center-of-mass system) as a function of center-of-mass scattering angle. Probable errors of the relative cross section are shown plotted with the points; these are based either on purely statistical errors or a conservative estimate of systematic deviations. The probable error of the absolute scale is ±3.0 percent.

[25] Lattes, Fowler, and Cüer, Proc. Phys. Soc. London **59**, 883 (1947).

V. ESTIMATE OF ACCURACY

A. Errors Affecting the Relative Cross Section

In discussing the errors in this experiment it is necessory to distinguish those errors which affect the accuracy of the absolute cross section only from those affecting the angular distribution. Let us discuss the latter first.

1. Statistics

10,934 tracks have been tabulated. The number of subdivisions in angle is of course arbitrary and has to be chosen in accordance with the rate of angular variation of the observed cross section. If the data are tabulated in 4° intervals in the laboratory system (Fig. 15), then the maximum rate of variation per point is about two probable errors and therefore probably significant. At this angular interval the statistical probable errors vary from ±2.3 percent (at 43° laboratory angle) to ±3.3 percent (at 12° laboratory angle).

2. Reliability of Observers

About two-thirds of the tabulated tracks have been read by one of us (F.L.F.) and the remainder by the other author (W.K.H.P.) and Mrs. Sue Gray Al-Salam, to whom the authors are greatly indebted. To check the reliability of observers F.L.F. has re-read samples of plates read by other observers. The re-reading cannot be done in a manner which is completely independent of the first reading because it is impossible to reset the swath position to closer than about $\pm 5\mu$. This means that tracks which are near the edge of a swath might correctly be counted inside by one observer and outside by another. The method used was to scan along a swath until a good track is found and then to look at the other observers' data and see if they had counted this track. In tabulating tracks missed, allowance is made for tracks which start near the edge of a swath. It is felt that the number of tracks missed by both observers is less than one-half percent so that to a good approximation we may tabulate the difference between the first observer's count and both observer's count as being the number missed by the first observer. The results of the principal run are given in Table II. No systematic difference in angular distribution was discovered in the tracks missed.

3. Accuracy of Angular Measurement

It was shown in Section III that in the interval $10° \leq \theta_{lab} \leq 65°$, where the angle is determined by direct measurement, the probable error in θ_{lab} varies from $\Delta\theta_{lab} = \pm 0.3°$ at $\theta_{lab} = 10°$ to $\Delta\theta_{lab} = \pm 1.0°$ at $\theta_{lab} = 65°$. In the interval $65° \leq \theta_{lab} \leq 80°$, where θ_{lab} is determined from range measurement, $\Delta\theta_{lab} = \pm 0.23°$ at $\theta_{lab} = 65°$ and $\Delta\theta_{lab} = \pm 0.44°$ at $\theta_{lab} = 80°$. Owing to the slow variation of cross section with angle, the angular uncertainties do not contribute appreciably to the error in the relative cross section.

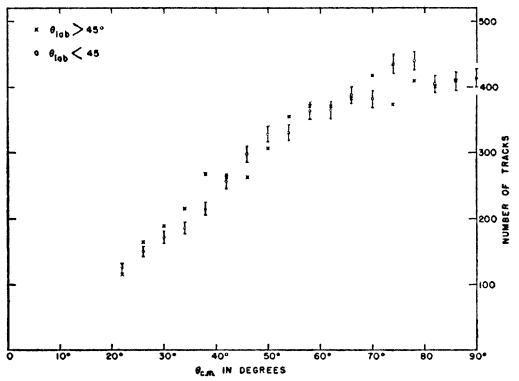

FIG. 16. Track counts plotted separately for laboratory scattering angle >45° and <45°. Equality between the count at a given angle and its complement serves as a criterion of like particle scattering.

4. Geometrical Errors

None of the geometrical errors discussed contribute to the uncertainty in relative cross section.

5. Impurities and Background

The total number of "confusable" tracks observed in the background runs was 0.7 percent with no significant angular correlation. Thus background effects to not appreciably contribute to the probable error of the relative cross section.

The impurity content can be estimated from the rate of rise of pressure with the chamber isolated and the rate of pure gas exchange. The results gives 4×10^{-5} for the maximum impurity content. Even at $\theta_{lab} = 10°$ the Coulomb contribution to the scattering yield due to the impurity (taken as $Z=8$) is thus only 7×10^{-4} of the observed proton yield.

All background effects, impurity scattering and systematic observational errors, are detectable by the fact that they presumably do not possess the symmetry about a laboratory angle of 45° characteristic of like particle scattering. Figure 16 shows the data plotted separately in the angular intervals $\theta_{lab} \gtrless 45°$. There is no statistically significant disagreement between the data in the two angular intervals. Nevertheless, the statistical error of any internal check of this kind is twice as large as the statistical error of the combined data. One can therefore conclude from the absence of any systematic dissymmetry that the effect of impurity scattering and background is not larger than the statistical error of the combined data; by the preceding arguments it is probably much smaller than this.

It appears as the result of this discussion that a conservative estimate for the probable error of the differential cross section is $\sqrt{2}$ times the statistical error of the combined data.

B. Errors Affecting the Absolute Cross Section

As was discussed in Section II-B the error is greatly reduced if the absolute cross section is obtained by

TABLE III. Data from individual plates. (The notation is that of Section II-B.)

Pair No.	Pair	Number of tracks	$\Sigma L/y^2$	Number of tracks weighted by scanned area and swath distance	$\frac{\delta Z}{Z}=\frac{N_1-N_2}{N_1+N_2}$	ϵ_Z percent
A	1	1127	10.94	103.0	0.1237	0.021
	2	1412	10.69	132.1		
B	1	1006	16.00	91.5	0.1766	0.044
	2	1449	11.08	130.8		
C	1	1299	11.24	115.5	0.0538	0.004
	2	1072	10.34	103.7		
					Mean error	0.023 percent

adding the tracks counted on symmetrically located pairs of plates. The basic formula for the absolute cross section is then

$$\left(\frac{d\sigma}{d\omega}\right)_{cm}=\frac{\Sigma N_t}{WN_pN_v\Delta(\cos\theta_{cm})}\times\frac{1}{\Sigma(LZ/y^2+Z^2)_1+\Sigma(LZ/y^2+Z^2)_2},\quad(20)$$

where ΣN_t represent the sum of all tracks counted in the increment $\Delta(\cos\theta_{cm})$ in plates 1 and 2. The summations in the denominator give the solid angle factor weight for each swath, this being necessary since L and y are different for each swath. We will now discuss the errors contributed by each factor in Eq. (20); these errors will be denoted by ϵ with appropriate subscripts.

1. Statistics

Owing to the fact that the observed differential cross section is essentially flat near $\theta_{\text{lab}}=45°$, the tracks in the angular range $40°\leq\theta_{\text{lab}}\leq 50°$ have been combined to give the absolute cross-section data. There are 1350 tracks in this angular range on which the computation is based, corresponding to a statistical probable error of $\epsilon_s=1.84$ percent.

2. Pressure Measurements

The pressure measurement is certainly accurate to 0.3 mm of Hg which corresponds to an accuracy of 0.2 mm of Hg in the reading of the mercury barometer and 2 mm in the reading of the oil manometer. This gives $\epsilon_p=0.04$ percent.

3. Temperature Measurement

The principal question as to accuracy of temprature measurement rests on the problem of temperature equilibrium discussed in Section II-C. It was concluded that equilibrium was established to within 1°C, corresponding to $\epsilon_T=0.3$ percent.

4. Errors in Beam Integration

(*a*) *Standard condenser.*—A polystyrene insulated condenser of nominal capacity 0.01 μf was sealed in a glass tube and calibrated against a General Radio Company standard condenser (certified accurate to 0.1 percent) by means of a ballistic galvanometer method. The calibration was made both before the runs and six months later; during this time a shift of 0.75 percent occurred. Owing to the slide-back system used no correction for lead and collecting cup capacity is necessary. We consider this equivalent to a 0.4 percent probable error.

(*b*) *Condenser voltage.*—The condenser voltage was measured by a standard cell-potentiometer method, accurate to 0.1 percent.

(*c*) *Condenser time constant.*—The condenser time constant was in all cases greater than 500 hr.; this corresponds to a possible error of 0.2 percent.

(*d*) *Secondary particles from collector.*—The tests made to check on secondary particles are described in the adjoining paper by Cork, Johnston, and Richman. It is concluded there that the effect of secondaries is less than 1.0 percent provided a proper high retarding voltage is used. We shall use a 1.0 percent probable error for this effect. Combining the integration errors we obtain: $\epsilon_I=1.1$ percent.

5. Plate Separation

The error in plate spacing is defined by the machining tolerance of ± 0.0005 in. of the plate holder, 0.001 in. can thus be considered a limit of error and 0.0005 in. a probable error. The plate thickness measurement has a probable error of ± 0.0004 in. These errors combine quadratically to give $\epsilon_D=1.11$ percent.

6. Swath Separation in the y Direction

The error in plate edge-to-edge separation was measured to a probable error of ± 0.002 in. A swath is about 0.006 in. wide, so the value of y in the cross-section formula has a maximum uncertainty due to swath width of ± 0.003 in. Taking half of this for the probable error we find $\delta_y=\pm 0.0018$ in., whence $\epsilon_y=0.36$ percent.

7. Beam Centering Errors

As has been discussed in Section II-B the errors due to beam centering as affecting the cross section derived from adding counts in pairs of plates can be calculated from the difference in the counts in pairs of plates. In Table III 7843 counts from the individual plates as obtained in Run 37 have been listed. This source of error is thus seen to be negligible.

8. Swath Width

The swath width of $W=127\mu$ has a probable error of $\pm 0.5\mu$ or 0.40 percent.

9. Other Geometrical Errors

Other geometrical errors which have been considered and found negligible are: (a) errors caused by lack of centering in the y direction; (b) errors caused by "scattering out" of tracks; (c) errors in knowing length of swath L.

10. Observational Errors

The observational error is much more serious in the case of the absolute cross section than it is in the case of the relative cross sections. The tabulation in Section IV-A shows that different observers diverge by a r.m.s. amount of 1.7 percent. This has been taken as the observational probable error in absolute cross section. The absolute cross section has a correction of -0.1 percent applied to take care of the tracks missed and duplicated. (See Section V-A-2.)

11. Uncertainty in Background

A correction of -0.7 percent has been applied as a background correction. The probable error of this correction is taken as ± 0.5 percent.

12. Combination of Errors

If the errors enumerated above are combined quadradically we obtain: $\epsilon_{\text{absolute cross section}} = \pm 3.0$ percent.

VI. RESULTS

A. Summary of Runs

Table IV summarizes the four runs upon which these results are based. We list all of the data taken for each run except for the detailed breakdown of the number of tracks counted in each angular interval.

B. Absolute Cross Section

The absolute cross section for a set of paired plates is calculated from Eq. (20) with N_p expressed in terms of the condenser voltage and capacitance, and N_v expressed in terms of pressure and temperature. The number of tracks observed in the two plates between $\theta_{cm} = 80°$ to 100° is weighted by the solid angle factor as previously explained. The results thus obtained for the three sets of plates are then weighted according to their statistics and averaged giving the final result. For this calculation we have used the results of Run 37 only since the total charge collected in the earlier Run 28 was not known to better than about two percent. We thus obtain 15.94 ± 0.48 millibarn/sterad. for the absolute value of the cross section at $\theta_{cm} = 90°$ at an energy of 29.4 ± 0.1 Mev.

C. Angular Dependence

The angular dependence of the cross section is found by dividing the number of tracks counted in each angular interval on all the plates by the sine of twice the laboratory angle at the center of each interval respectively. This gives relative values for the cross section which are then normalized to the absolute value over the interval $40° \leq \theta_{\text{lab}} \leq 50°$. The probable errors to be attached to each value thus obtained depend only on statistics as previously explained. The results are shown in Fig. 15.

VII. DISCUSSION OF RESULTS

A detailed analysis of these data has been undertaken at this laboratory by Christian and Noyes[26] and is being presented in an adjoining paper. It might be well here to discuss some of the conclusions.

In all prior $p-p$ scattering work only S-wave contributions were obtainable but in the interpretation of the low energy work[27] it has been frequently attempted to interpret small repulsive P-interactions from the data. The principal result of the present work is the approximate absence of any apparent higher angular momentum contribution, be it caused by a real absence of such terms or a fortuitous masking effect. The fact that this work disagrees even qualitatively from the

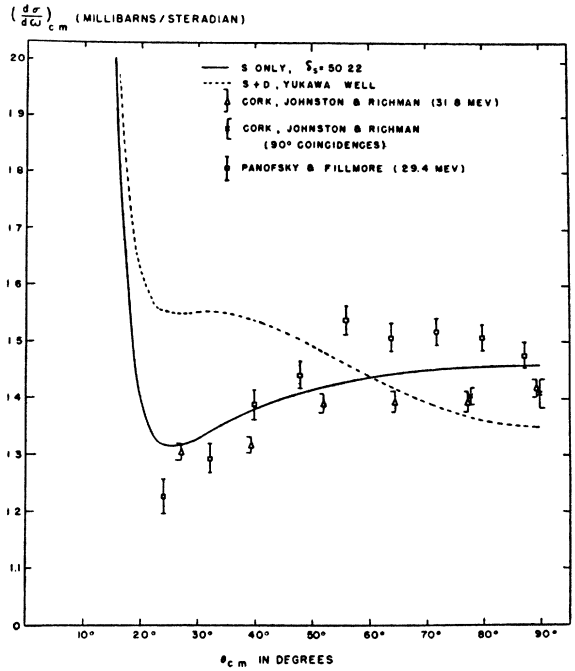

FIG. 17. Differential cross sections of Panofsky and Fillmore and of Cork, Johnston, and Richman (see reference 20) plotted together reduced to a common primary energy of 32.0 Mev by an assumed $1/E$ dependence of cross section. The two sets of data are *not* normalized but the absolute cross-section values are independent. Two theoretical curves (kindly supplied by Mr. P. Noyes) are shown: (a) pure S scattering using $\delta_s = 50.22°$; (b) total singlet scattering ($S+D$ scattering) using a Yukawa well and the same S phase shift. (Note suppressed zero of ordinate scale.)

[26] R. Christian and P. Noyes, Phys. Rev. **79**, 85 (1950).
[27] See, e.g., L. I. Foldy, Phys. Rev. **72**, 125, 731 (1947); also reference 10.

TABLE IV. Summary of runs.

Run No.	Date	Type of run	Time for pressure to reach 10^{-4} mm (sec.)	Temp. (°C)	Pressure (mm of Hg)	Charge collected (coulombs)	N_s	N_p	Total No. tracks counted
28	2–7 –49	Scattering	5.2	18	747.6	1.6×10^{-8}	4.95×10^{19}	1×10^{11}	3091
37	3–11–49	Scattering	3.9	24.3	757.0	1.401×10^{-8}	4.912×10^{19}	0.8745×10^{11}	7843
33	2–26–49	Background	1.2	—	10^{-4}	1.5×10^{-8}	—	0.94×10^{11}	12 confusable
38	3–12–49	Background	3.0	21.5	761.0	1.59×10^{-8}	4.98×10^{19}	0.99×10^{11}	37 confusable

expected results is the reason that this work is being presented now in its admittedly unfinished form.

At this energy also D-wave contributions should be appreciable and in particular an angular distribution including the singlet D-interaction can be computed from the low energy data, since the range and depth of the potential are known to good precision. The apparent absence of this contribution also means that there is either a very fundamental difficulty with the analysis of the data by a static potential or that a masking effect occurs. Christian and Noyes have investigated this point and have shown that it is formally possible at least to produce such a masking by a strong tensor interaction. Also such a strong tensor term accounts, at least qualitatively, for the large absolute differential cross section observed at a primary proton energy of 340 Mev[15] and 240 Mev.[14]

Figure 17 shows the data as obtained here plotted together with those of Cork, Richman, and Johnston.[20] Note that the primary proton energy of the two experiments differs by 2.4 Mev so that the absolute cross section measurements can be considered to be in agreement with an approximate $1/E$ variation of differential cross section and the assigned probable errors of the two experiments. It is also felt that the differences in shape between the two curves cannot be considered significant.

Figure 17 shows also the curve computed on the basis of singlet S and D interactions alone; it is thus seen clearly that neither of the experimental data are compatible with a central force static potential.

VIII. ACKNOWLEDGMENTS

The authors have benefited by the active cooperation of many members of this laboratory. In particular, thanks are due Mr. Al Kaehler for mechanical design, Mr. Lee Aamodt for construction of the integrator, Mrs. Sue Al-Salam and Miss Amy Bates for aid in reading and tabulating tracks. We have enjoyed the cooperation and advice of Messrs. Cork, Richman and Johnston in discussing our mutual difficulties, but it is believed that the results can be considered fully independent. The bombardments were carried out by the linear accelerator crew under the direction of Mr. Saul Lissauer.